Review Article

Chemical Characteristics, Motivation and Strategies in choice of Materials used as Liver Phantom: A Literature Review

Muntaser S. Ahmad[1], Nursakinah Suardi[1]*, Ahmad Shukri[1], Hjouj Mohammad[2], Ammar A. Oglat[3]*, Azzam Alarab[4], Osama Makhamrah[2]

[1]Department of Medical Physics and Radiation Science, School of Physics, Universiti Sains Malaysia, Malaysia, [2]Department of Medical Imaging, Faculty of Health Professions, Al-Quds University, Abu Deis - Main Campus, Jerusalem, [3]Department of Medical Imaging, Faculty of Allied Health Sciences, The Hashemite University, Zarqa, Jordan, [4]Department of Medical Imaging, Faculty of Allied Medical Health, Palestine Ahlyia University, Bethlehem, Palestine

Abstract

Liver phantoms have been developed as an alternative to human tissue and have been used for different purposes. In this article, the items used for liver phantoms fabrication are mentioned same as in the previous literature reviews. Summary and characteristics of these materials are presented. The main factors that need to be available in the materials used for fabrication in computed tomography, ultrasound, magnetic resonance imaging, and nuclear medicine were analyzed. Finally, the discussion focuses on some purposes and aims of the liver phantom fabrication for use in several areas such as training, diagnoses of different diseases, and treatment planning for therapeutic strategies – for example, in selective internal radiation therapy, stereotactic body radiation therapy, laser-induced thermotherapy, radiofrequency ablation, and microwave coagulation therapy. It was found that different liver substitutes can be developed to fulfill the different requirements.

Keywords: Liver phantoms, radioembolization, radiofrequency ablation, selective internal radiation therapy, tissue-mimicking material

Introduction

Liver is considered as the largest solid organ and gland in the human body. It is an essential organ with a lot of functions such as metabolism center producing nutrients and important vitamins, as well as playing an important role in the and excretion of waste metabolites.[1] There are several pathologies that can affect the liver such as liver fibrosis, fatty liver, liver cirrhosis, and hepatocellular carcinoma (HCC). The loss of total liver function may lead to death within minute days, indicating the importance of the liver.

Currently, one of the fastest growing areas of medicine, both in development and research and in clinical settings, is medical imaging. Medical imaging plays a significant role in the care of the patient and is constantly used in the management of health and disease.[2] For example, it is used in the diseases detection, provide an optimal treatments through surgical interventions, and monitoring of treatment effects. During surgical interventions, the imaging modalities must be easily obtainable, and it is preferable to provide real-time images for optimum orientation. Instead of using human tissues, phantoms that mimic human or animal tissues – tissue-mimicking materials (TMMs) – are required for giving more information's of the guided image in therapeutic interventions and diagnostic imaging techniques.[3]

Over the past decade, the attention to patient safety has increased. Furthermore, the efforts toward risk reduction have increased. Thus, the simulation steps are considered an important stride in clinical training. Especially in diagnostic and interventional procedures, suitable training is allowed for novices to promote and improve medical practice. For safety purposes, training is performed on interventions that are directed to biopsy or ablation on simulators. The use of simulators has brought many benefits such as improvements in the learning experience and increased patient safety.[4] For this reason, phantoms have been developed.

Address for correspondence: Dr. Nursakinah Suardi, School of Physics, Universiti Sains Malaysia, 11800 Penang, Malaysia.
E-mail: nsakinahsuardi@usm.my

Received: 15-01-2019 **Revised:** 26-02-2019 **Accepted:** 24-05-2019 **Available Online:** 28-01-2020

Access this article online

Quick Response Code:

Website: www.jmuonline.org

DOI: 10.4103/JMU.JMU_4_19

How to cite this article: Ahmad MS, Suardi N, Shukri A, Mohammad H, Oglat AA, Alarab A, *et al*. Chemical characteristics, motivation and strategies in choice of materials used as liver phantom: A literature review. J Med Ultrasound 2020;28:7-16.

A phantom made of tissue equivalent materials is considered an important factor for quality control of diagnostic equipment. It is essential to manufacture synthetic materials which are used in phantoms in a controlled way to be almost equivalent to human tissue.[5] Anatomical phantoms are greatly applied in molecular imaging for the quantitative and qualitative estimation of image quality (IQ); these phantoms are predominantly expensive and hardly specific to the cohort of interest or patient.[6]

Given this scenario, this study was undertaken to review the materials which are used to fabricate the liver phantoms. Also, it provides an information's about the phantom characteristics for each medical imaging modality.

Fabrication Materials

Several materials have been used to develop an ideal liver phantom that could achieve success in liver procedures. A framework should be completely uniform in their components and can be formed in three-dimensional (3-D) frameworks. The material should mimic the morphology and structure of the real liver organ to obtain the 3-D. Thus, many substances have been checked to achieve the liver phantom realization that can be stable over time. The materials that can be used are completely harmless and do not need to control by their temperature. The most common substances used for phantom fabrication are polyacrylamide (PAA), carrageenan, polysaccharide, agar, agarose, polyvinyl alcohol (PVA), polyurethane, gelatin and silicone, commercial rigid plastics, and elastomeric (rubber-like) materials. These materials have many properties which can be summarized as follows.

Polyacrylamide gel

The main constituent of a tissue-simulating compound (TSC) was acrylamide C_3H_5NO; when water is added to it, the PAA gel is produced.[7] PAA gel is a solid, optically transparent, solid elastic and is easily formed into the desired shape. This provides the possibility of working with multilayered samples, where each layer has a different character due to water concentration. When water evaporation is stopped by phantom sealing, the electrical characteristics and properties of magnetic resonance imaging (MRI) are stable at the right time.[8]

The PAA phantoms can be used for 5 months without significant difference in its characteristics. The phantom must be stored in sealed glass tubes. PAA gels are appropriately moldable, inexpensive, and not affected by temperature fluctuations.

Carrageenan gel

Carrageenan is a polysaccharide that is taken from seaweed, with properties similar to those found in agar. It consists of saccharides with molecular weights of 100,000–500,000, most of which are galactose and 3,6-anhydrogalactose. However, it is considered more flexible and resistant to the crushing of the agar gel, allowing the production of large phantoms in a variety of different shapes. Carrageenan is safe and inexpensive. This material can be used as MRI phantoms; however, when carrageenan concentration reaches a level that can produce the hard phantom, the T2 relaxation time would be longer than that of human tissue.

Polysaccharide gel

These are high molecular weight substances consisting of simple sugar or sugar derivatives. The molecular structure of the gel forms part of the tissue cell walls, intercellular coating spaces, and connective tissue. It contains one to six C-OH groups per monomer unit, which provides wide sites for hydrogen to bond in hydrated gels. When other materials such as agar or animal gelatin (hydrated gels) are added,[9] polysaccharides can be applied for MRI tissue equivalents. Unfortunately, the polysaccharide gel is unstable with time and loses its properties in a few weeks.

Agar gel

The agar gel has some characteristics such as water–gel structure and is characterized by a restricted movement of the bonded molecule and free water; it allows normal biological functions of water necessary for cell growth. Moreover, some of the internal components of living organisms are like the gel. However, the agar is considered a hydrophilic, organic material and this type of materials has disadvantages because it is a good medium to grow microbes. Thus, the acoustic characteristic will be changed with time.[5] In addition, the agar gel can be easily formed and handled by changing the temperature; at the same time, it is easy to cool down at room temperature. Consequently, the gel preparation and reproducibility are fairly simple.[10]

Agarose gel

Agarose is a polysaccharide, generally extracted from certain red seaweed. It is a linear polymer made up of the repeating unit of agarobiose [Figure 1], which is a disaccharide made up of D-galactose and 3,6-anhydro-L-galactopyranose. Agarose is one of the two principal components of agar and is purified from agar by removing the other agar's component, agaropectin.[9] This material has properties of independence in both temperature and magnetic flux density. In addition, it is characterized by easy manufacturing and configuration and does not change its characteristics over time.[11]

Polyvinyl alcohol-based tissue

The polyvinyl alcohol (PVA)-based tissue known as cryogels is nontoxic, widely used in the industrial compound, usually in glue and food packaging. This material is a sticky liquid consisting of 10% of PVA dissolved in water, so it can be

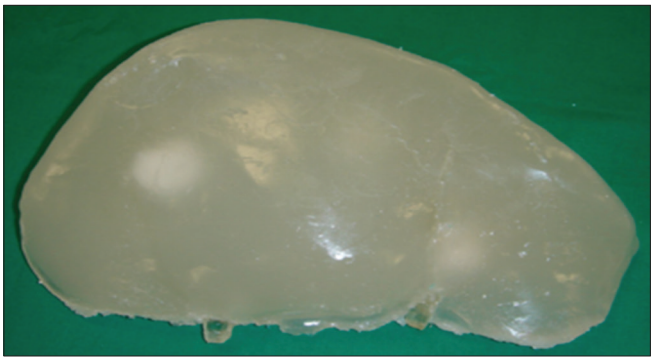

Figure 1: Phantom appearance: agarose-candle gel anterior view[12]

used in a gel which has tissue-mimicking properties by the fashioning of crystallites through repeating freeze-thaw cycles [Figure 2]. The cryogel has many benefits such as longevity, low-cost, and structural stability over a long period and needs less components than agarose and gelatin-based tissue. The preparation of this material entails control of temperature, and diverse 12-h freezing thaw cycles. The cryogel is easily handling with gelatin agar which shows well adapted for intravascular elastography. This material can be used for blood-mimicking fluid (BMF) in MRI experiments besides using as anatomical specimens.[12,13]

Polyurethane gel

The gel is produced by reacting a polyurethane, this material having liquid alkaline with oxide chain at room temperature. This material has a high elastic recovery without decreasing their strength, and it is also resistant to bacterial infection. However, this material is problematic in phantom production, due to the complex design of molecular of the polyurethane gel.[5] Because this material has an excellent resistance with low viscosity, it can be used in various casting materials.[13] A polyurethane model with anthropomorphic liver is shown in Figure 3.

Gelatin-alginate

Alginate seaweed is taken from brown algae. It is a polysaccharide with ionic properties, and alginate can combine with gelatin to form a more stable system. The producing solution is complex and can be cooled below 25°C to form opaque gel. This material has complexity in its structure; it can be stored beneath water without requiring elaborate protection gelatin and can be used in a short term because the water evaporates rapidly from solution at room temperature and the structure changes with refrigeration.[14]

Silicone polymer, room-temperature-vulcanizing silicone

Silicones, also known as polysiloxanes, are polymers that do not have carbon as a part of its basic structure. This material has many properties such as robustness, good stability, and easy to fabricate. Thus, the phantom can be used in the vessel's molds and also can be used to keep the moist of the phantom. Therefore, the phantom can easily be transported from one place to another without being damaged. In the same time, it conserves the phantom to be used in the long term.[15] Room-temperature-vulcanizing (RTV) silicone is a type of silicone rubber made from a system consisting of two compounds (a crosslinker and a catalyst), available with hardness range from very soft to medium. RTV silicones can be handled with a catalyst made up of platinum or tin compound such as dibutyltin deliberate. In comparison to hydrogels, the silicon is not affected by various dehydration factors, so the temperature does not affect silicon significantly as compared to its effect on halogens that are clearly affected by the temperature. The problem of this material is mismatching with biological tissues for acoustical properties.[4]

Polyethylene glycol diacrylate-based hydrogel

A dual-function molecule (average Mn 700) can be polymerized by free radicals such as water solution which is derived from suitable photo-initiators. This solution can be prepared by resolving the photo-initiator in polyethylene glycol diacrylate by softly stirring the solution (concentration 2% w/v polymer) at room temperature until it reaches to the homogeneous mixture. After that, add the distilled water slowly to the solution until it reaches to 15% weight/volume of the polymer.[16]

Commercial rigid plastics

Rigid plastics can be defined as any material used for polymers. This type of plastic has high density and molecular weight; moreover, it has a transition temperature more than the room temperature (>25°C). However, there have been many items used as three-dimensional (3-D)-printed phantoms to mimic human organs. Some examples are polylactic acid, acrylonitrile butadiene styrene, and thermoplastic filaments. The elastic properties of these items differ from other normal tissue due to the difference in the degree of stiffness and the structure. Furthermore, these plastic items have a stability in shape and composition and can be used over the long term [Figure 4].[3]

Elastomeric (rubber-like) materials

Elastomeric materials can be used in a wide range of applications and depend on several processes: First – PolyJet process which used suitable material called Tango™ family (Stratasys); second – thermoplastic elastomer filaments which used suitable materials called NinjaFlex® (NinjaTek) and SemiFlex™ (NinjaTek); finally – FDM printing which used

Figure 2: Polyvinyl alcohol cryogel-liver phantom[15]

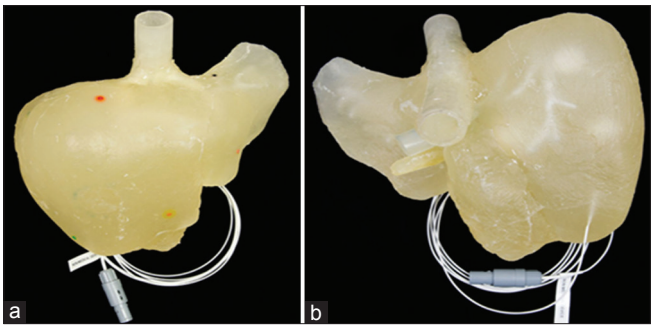

Figure 3: Anthropomorphic liver using polyurethane (a) anterior view and (b) posteroinferiorly view[16]

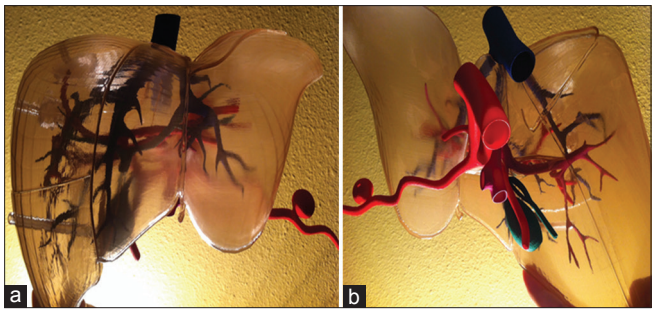

Figure 4: Plastic three-dimensional-printed model of the liver: (a) anterior view and (b) poster inferiorly view[20]

PolyFlex™ (Poly-maker). Thus, these materials are very close to the actual organs.[3] Table 1 provides a summary of advantages and disadvantages of the most common materials used for phantoms fabrication as discussed in this article.

For 3-D printer, the most commonly used substances in the manufacture of liver phantom are Tango Black,[17,18] wax,[19] plastic,[19] polymax,[20] and silicone gel.[21]

There are also some materials which were used for fabrication of liver phantoms to achieve specific purposes. The materials used to mimic the fatty liver tissues are called glucose solution combined with tertbutyl alcohol in water,[22] whereas the materials such as butanol, methanol, glycerin, KNO_3, and NaCl were used to fabricate liquid tissue surrogates.[23]

Phantoms Properties-Related Modality

TMM properties should exhibit the same for human tissue at room temperature.[24] In the same time, the organ model properties should be compatible with the real-organ properties, such as human densities, anatomy size, and weight. The phantoms should be constructed from nontoxic materials, and at the same time, nondegradable over time, it must also maintain its structure and reproducible, and it should be easy to handle. Finally, the materials used in manufacturing are cheaply priced . There is a different level of similarity between phantom components, and the biological tissues can be specified in order of medical modalities as the following summarized.

Computed tomography

The phantom materials (TMM) for use in computed tomography (CT) must exhibit properties of the same CT numbers.[25] For example, the Hounsfield units mean that the same linear attenuation coefficient (AC) of the human tissue, and an attenuation measurement is used to quantify the fraction of radiation removed in transmitting through an amount of a particular material of thickness x. Attenuation is given by:

$$I_x = I_0 e^{-\mu x} \quad (1)$$

where I_x is the intensity of X-ray with the body after X-ray beam path, I_0 is the x-ray intensity before interact with the body, x is the object thickness, and μ is the linear AC of the object.[26] The linear AC depended on many factors such as the density of materials, the effective atomic number, and the energy of the radiation. The effective atomic number (Zeff) can calculated by:

$$Z_{eff} = \sqrt[x]{w_1 Z_1^x + w_2 Z_2^x + \ldots + w_n Z_n^x} \quad (2)$$

where w_n is the fraction of the total number of electrons associated with each element and Z_n is the atomic number of each element.[27]

The electron density and mass density are the other factors need to calculate for CT material fabrication, the ρe of the two materials was computed from its mass density (ρm), and its atomic composition according to the formula:

$$\rho e = \rho m \times NA \times \left(\frac{Z}{A}\right) \quad (3)$$

where NA is Avogadro's number, Z is the atomic number, and A is the atomic weight obtained from chemical analysis test. The Hounsfield unit for most soft tissue except fat is between 20 and 90 at effective X-ray energy 120–140 kVp, whereas the fatty tissue reaches to −100. The most commonly used substances in the manufacture of liver which are subject to CT are agar[28,29] agarose gel,[30] and plastic foam[31-33]

Ultrasound

The TMMs for use in ultrasound (US) ought to have the same acoustic properties, such as velocity of sound, the AC, acoustic impedance (Z), and backscatter coefficient.[27-30] Moreover, the most commonly used substances in the manufacture of liver which are subject to US are gelatin,[34-36] poly (vinyl alcohol) cryogel,[37] polyurethane gels,[5] and agar.[38]

Acoustic velocity and speed of sound

The velocity at which a small disturbance will propagate through the medium is called acoustic velocity or speed of sound. The acoustic velocity (c_s) is related to the change in pressure and density of the substance and can be expressed as:

$$c_s = \left(\frac{dp}{d\rho}\right)^{\frac{1}{2}} = \left(\frac{k_s}{\rho}\right)^{\frac{1}{2}} \left[\frac{m}{s}\right] \quad (4)$$

where dp is the change in pressure in Pascal (Pa), dρ is the change of density in Kg/m^3, and k_s is the coefficient of stiffness or the modulus of bulk elasticity.[39]

Attenuation coefficient

The AC can be calculated at the only frequency of 1 MHz using following formula, mentioning this formula only to provide magnitude for mimic materials:

$$\alpha_s = \alpha_w - \frac{1}{\Delta x}\left[In\, A_s - In\, A_w - 2In(1-R)\right] \quad (5)$$

where A_s is the US pulse amplitude, A_w is water amplitude, and R is the coefficient of acoustical reflection at the interface between material and water itself. The R magnitude can be calculated by this formula:

Table 1: Advantages and disadvantages of chemical materials for phantom fabrication

Material	Advantages	Disadvantage	Image modality used
PAA gel	Elastic and easily formed Used for multi-layered samples Inexpensive ↓ Temperature fluctuations	Time stability for 5 months Requires storage in sealed glass tubes	Suitable for MRI device
Carrageenan gel	Easily mold to different shapes Inexpensive	The relaxation time different. During hardness	Suitable for MRI device
PAAG gel	Provides wide sites for hydrogen	Properties affected by temperature	Suitable for MRI device
Agar gel	Hydrophilic organic materials Easily formed by temperature	Restricted movement in free water Good media to grow the bacterial organism	Suitable for MRI, US, CT and scintillation camera imaging
Agarose gel	Independent of temperature Used in different shape Stable in long period	More complicated components than agar	Suitable for MRI and CT
PVA (cryogel)	Low cost price Stable in long time Easily handling		Suitable for MRI and US
Polyurethane gel	High elastic recovery Resistance to bacterial infection Low viscosity	Complex in molecular design	Suitable for US
Gelatine-alginate	↑ Stability Store beneath water	Complex structure Lack of longevity	Suitable for US and scintillation camera
Silicone polymer, RTV	Robust material ↑ Stability for long time Easily formed	Mismatching with biological tissues	Suitable for CT
PEGDA	Easily formed	Complex structure	Suitable for US
Commercial rigid plastics	↑ Stability in shape ↑ Stability for long time	Stiffness more than normal tissue Complex structure Need specific device	Suitable for US, CT and scintillation camera imaging
Elastomeric (rubber-like) materials	Good flexibility Good elasticity	Complex structure Need specific device	Suitable for MRI and US

MRI: Magnetic resonance imaging, CT: Computed tomography, US: Ultrasound, RTV: Room-temperature-vulcanizing silicone, PEGDA: Polyethylene glycol diacrylate, PVA: Polyvinyl alcohol, PAAG: Polysaccharide Gel, PAA: Polyacrylamide, ↓ Decreasing, ↑ Increasing

$$R = \frac{Z_2 - Z_1}{Z_2 + Z_1} \quad (6)$$

where Z is the acoustic impedance that depends on the density of material and velocity of sound in this material.[35] The sound speed has a value of 1540 ± 15 m/s, Acoustic impedance is (1.6±0.16) 10^6 kg m^{-2} s^{-1}, and the AC in a real liver is approximately 0.5–0.7 ± 0.05 dB/cm for 1 MHz frequency.[40]

Backscatter coefficient

The backscatter coefficients in US can be controlled by appending small concentrations of glass diameter scatters. Some of the physical properties are taken into consideration to be BMF such as the concentration of volume of acoustic backscattered, the size of the scatterer, the compressibility between the fluid scattering and surrounding fluid, the density of the fluid, the viscosity, and finally the acoustic properties.[33,41-43] The backscatter coefficient can be estimated by using this equation:

$$BS(f,z) = \frac{S_S(f,z)}{S_R(f,z)}\ BS_R(f,z)\,A(f,z) \quad (7)$$

where S_s and S_R are the sample spectra and reference phantom spectra, BS_R is the reference phantom backscatter, A is a compensates function for attenuation along the propagation path, f is the frequency of ultrasonic wave, and z is the region depth of analysis.

If using different ultrasonic frequencies, the backscatter coefficient can be calculated by the integration as defined in equation (8):[44,45]

$$iBSC = \frac{1}{f_2 - f_1}\int_{f_1}^{f_2} BS(f)\,df \quad (8)$$

where iBSC is the integrated backscatter coefficient, f_2 and f_1 are the higher and the lower frequency values in the employed range, respectively.

Scintillation camera imaging

For use the scintillation camera imaging, the TMMs should exhibit the same sensitivity, spatial resolution, count rate linearity, and contrast recovery of some radiopharmaceuticals such as ^{99m}Tc, ^{90}Y, and ^{166}Ho, in the following these characteristics summarized.[46] Therefore, the most commonly used substances in the manufacture of liver which are subject to scintillation camera are gelatin[14] and acrylic plastic material.[18,47-49]

Calibration factor

Calibration factor (CF) is determined by the ratio between the average count rate of the counts number. The average counts per second (cps) are the activity of the source inside the phantom in Becquerel (Bq). The CF can be calculated using following formula:

$$CF_{cps/Bq} = {cps}/{A} \quad (9)$$

where cps is the net count rate (averaged cps of the phantom) and A (Bq) is ^{60}Co activity content of the liver phantom.[50]

Sensitivity

The sensitivity can be defined as the smallest amounts of activity that can be detected (minimum detectable activity [MDA]), and it is related directly to the image noise. It can be measured by filling a thin cylinder layer with radiopharmaceutical and compared the activity of the cylinder with radiopharmaceutical activity that was previously calibrated to the cylinder. The sensitivity (S) (cps/Mbq) can be calculated as the total number of counts in the field of view, divided by acquisition time times activity.[49] The MDA is based on calculation of the minimum detectable intake (MDI) and minimum detectable effective dose (MDED). The calculation was used under the realistic internal exposure scenario. Thus, the MDA is calculated as the follows:

$$MDA = \frac{4.65\sqrt{N}}{CF \times T} + \frac{3}{CF \times T} \quad (10)$$

where N is the total background counts of the region of interest and t is time of count.

The MDI is a part of MDA and depends on the exposure and the time of intake, and it can be calculated with the following formula:

$$MDI = \frac{MDA}{m(t)_{inh}} \quad (11)$$

where MDA in Bq, and m (t) is the retention fraction in the compartment of interest Bq/Bq.

While the MDED can be calculated by using the following equation:

$$MDED_{Bq} = MDI_{inh} \times e(g)_{inh} \quad (12)$$

where MDI in Bq, and e (g) is the dose coefficient which have a unit mSv/Bq.[50]

Spatial resolution

Spatial resolution can be defined as the ability of the system to detect the smallest distance between two adjacent objects as two separated points, and these points have a small activity accumulation. The detail and sharpness measurements of the scintillation camera image depend on the number of light photons statistically which collected from scintillation events and also depend on collimator efficiency. The typical values of spatial resolution are 2.5–3.5 mm. Spatial resolution can be quantitatively evaluated by of the point-spread function or line-spread function.[27]

Count rate linearity

In high-rate counting, this phenomenon that the probability to record two events at the same time is higher is known as pulse pile-up. It depends on losses counting and image distortion, and it is determined by total-spectrum counting rates. With a dead time of 5 μs, the counting losses reach 20% for a counting rate of 4×10^4 cps.[9]

Contrast recovery

Contrast recovery is considered as an important factor, and it can be performed using a set of objects with different sizes and contrasts. The objects consisted of solids with different diameters sunken in different thicknesses filled with radioactive material at uniform concentration. It is helpful to detect the large lesions with low contrast and at the same time to detect the small lesions with high contrast.[51]

Magnetic resonance imaging

TMMs that use as MRI phantoms ought to have some special properties such as:

Different proton density of a material with similar relaxation times (T1 and T2) which obtain *in vivo* (human tissue)[10]

Should support times of relaxation in a uniform way with the ability to change times TI and T2 independently[11]

Must be strong enough with stable in chemical and physical properties and this property must not be changeable with heat[52]

The pH and electric conductivity (circuit properties, power transfer) are similar to the soft tissue; in the same time, equivalence for the internal electromagnetic power deposition[8]

The variation of magnetic flux density and the temperature must be changed with respect to T1 and T2.[53]

For the electromagnetic equivalent, the materials are required that the real and imaginary parts of electrical permittivity (and magnetism) be equal to the specificity of the fabric to be simulated. The thermal equivalence is also required, and the materials should also include a heat capacity and conductivity equals that in the tissue. This needs constant of the thermal time of the material; materials with low temperature and low conductivity are the preferred materials for use in MRI.[7] Therefore, the most commonly used substances in the manufacture of liver which are subject to MRI are poly (vinyl alcohol) cryogel,[54-56] agar[57,58] agarose,[11] polyurethane,[59,60] and carrageenan[52,61] Table 2 shows the main properties of the TMM in the different medical imaging modalities.

Purposes of Phantoms

Diagnostic purposes

The phantoms are used in research of medical imaging to replace real tissues and in studies where the *in vivo* models are inadequate. Phantoms models can be designed on anatomical features, such as liver organ lobes, vascular vessels, and tree

Table 2: Fabrication material characteristics under the medical imaging modalities

Modality	Specific characteristic
CT	Linear attenuation coefficient
	Effective atomic number
	Electron density
US	Velocity of sound
	Attenuation coefficient
	Acoustic impedance
	Backscatter coefficient
Scintillation camera imaging	Sensitivity
	Spatial resolution
	Count rate linearity
	Contrast recovery
MRI	Relaxation time T1 and T2
	Uniform relaxation times
	Chemical and physical stability
	pH and electric conductivity

MRI: Magnetic resonance imaging, CT: Computed tomography, US: Ultrasound

vessels. The purposes of phantoms are differently depends on the procedures which needed, in the following paragraphs will discuss these aims with some details.

The liver phantom is needed for novices to provide training in diagnostic and interventional procedures. However, the proper training of novices authorizes to improve and develop their practices. It starts with novices of the phantoms to develop the abilities to deal with perfect handling before applied these practices on the real patient such as percutaneous biopsies and liver resection.[62] Thus, the patient safety increased, the risk of mistakes, and accidental injury of the liver vessels are reduced.[4] Moreover, because of the complicated design of the liver anatomy (organs, bile ducts, hepatic arteries, portal veins), the targeting accuracy must be improved. Thus, the steerable needle insertion were developed to improve the effectiveness of needle by using the anthropomorphic liver phantom and different modalities such as CT and US.[13,32]

The specifically designed phantoms can help to increase the quality assurance of patient reporting and treatments and provide perfect trial data collection. Its importance relies where radiotherapy clinical trials especially on dosimetry inter-comparison procedures, treatments precision, and terms which required complexity.[63] The phantom studies were used to assess the radiation dose and improved the IQ through using noise reduction technique specially for obese patients. In addition, the phantoms were used to achieve the maximum low-contrast detectability in CT modality.[41-43]

Another aims of the phantom possesses is to build a new reconstruction methods by developing the suitable algorithms especially in CT for several reasons: to evaluate the lesions, to improve the pathology visualization and achieved by developing different reconstruction techniques, to evaluate the effect of the iterative reconstruction on the contrast noise ratio, to evaluate the accuracy of dual-energy CT in diseases detection,[64] to develop the anatomical accuracy detection,[65] and finally to assess the virtual mono-energetic images to detect the hyper-density lesions[66] or the hypo-density lesions.[67] In the same time, the algorithms can be used in positron emission tomography scan to compensate the motion artifact through patient breathing.[68]

Otherwise, phantoms are fundamental to investigations of elastic imaging. For example, to visualize the strain image structures and tissues deformity that needs a precise knowledge of tissue changing when tissue undergoes to the strain and stress fields of a mechanical stimulus. In the acoustic strain estimates, the signal to noise ratio significantly reduces with scatters movement out of the image within the pulse volume or any vary distortion over time. Thus, the phantoms which mimic elastic and acoustic properties of the real human tissues are considered most effective methods to assess the data acquisition and task performance.[69]

In addition, the phantoms have been utilized to examine and evaluate the liver elasticity (Son-elasticity), and the evaluation of the tissue elasticity was done by using transient elastography and real-time tissue elastography. The elasticity of the tissue has been made known to the commercial US phantom,[69] which it provides elastic and structural measurements utilizing noninvasive medical US imaging scan. According to clinical (*in-vivo*) studies, the US elastography can improve the diagnostic rules and decisions for multiple diseases such as muscle problems, cardiovascular diseases, and tumors. The suitable method for measuring the tissue elasticity is to propagate impulse through the skin and to monitor gentle pressure using the US probe while imaging for a few seconds.[62] Then, the strain and a 2-D elasticity image of a few centimeters depth is measured and obtained.

Moreover, the relationship between impulse mean velocity and the liver stiffness is directly proportional. Hence, the liver connective tissue can be evaluated, and by utilizing a specific algorithm known as extended combined autocorrelation method and the elasticity of liver tissue can be expressed in arbitrary units (a.u.). Further, the elastography process helps to detect the liver fibrosis.[70]

Therapeutic or interventional purposes

The phantom is useful for the surgeon, in the surgical navigation by providing detailed information for the position of the instrument in the body patients. For this reason, the image-guided liver surgery has concerned and developed in the recent years. Therefore, it can help to estimate the correct measurements for the position of the instrument.

An additional use of the phantom, it can estimate the system of augmented reality (AR) guidance for laparoscopic liver surgery. The AR system guides the surgeon throughout the procedure utilizing AR glasses. The system first application is for spine surgeries. However, this system can be used to provide multi-other procedures such as liver surgery. The system can

facilitate the minimal invasive surgeries and to reduce its complication rate, the AR glasses project the CT image on the real patient allowing the surgeon to see the liver components through the skin. In the most liver surgeries there is a need to resect the tumors inside the liver. Thus, the surgeon can plan in advance the needle site before surgery and then to project a functional guide on the patient for the tumor to guide the needle inside, so it inserts gently and safely into the liver to its correct position without touch the main vessels. The augment system is very helpful in the complicated cases especially when the anatomy is not very clear. The physiological motion of the patient through the breathing motion made a challenge for accurate placement of the needle.[37-39]

Moreover, the phantoms are essentially in the therapeutic strategies for cancer tissues which depend on the target location.[16] However, the therapeutic strategies have several methods, such as SIRT or radioembolization (RE), which is one considered as a micro-brachytherapy technique used to treat primary and metastasis malignant hepatic lesions by using the 90Yttrium-labeled microspheres.[71] SIRT is a targeted treatment for in-operable liver tumors that delivers millions of radioactive microspheres directly to liver tumors and most material used in achieving this technique is plastic material.[18] The phantoms were applied to see the efficiency of intra-arterial liver RE in the liver lesion treatment especially with small-sized HCCs.[49] An additional strategy is stereotactic body radiation therapy (SBRT) that can be used as an alternative to the standard treatment modalities for treating liver tumors,[72] and most material used in achieving this technique is Polyethylene.[73-75]

The phantoms are also applied for tumor thermotherapy methods such as laser induced thermotherapy. The idea of this type of treatment is applied with the thermal energy for the tumor tissue for period of time (seconds to minutes). Therefore, the cancer tissue starts to coagulate then becomes necrotic tissue.[40,76] The PAA gel is used in the application of this therapeutic technique.[77,78]

The phantoms have been applied into the electromagnetic tracked laparoscopic US that can be used for laparoscopic ablation for liver tumors which needs the high positional accuracy. Thus, this can allow an optimal reduction for tumor tissues[79] such as radiofrequency ablation technique, which is used to treat the primary malignancies and metastasis for the several small tumors in different parts of the liver that is not a good candidate for resection.[80] RFA is a minimally invasive treatment for cancer, and it is guided digital imaging such as MRI, CT, and US. Thus cancer cells are eliminated using needle electrode which have been guided through the various modalities mentioned above.

Other application in this field is microwave coagulation therapy (MCT)[81] which was applied using gelatin material.[82] The tumor tissue can exist a several millimeters below the liver surface, and the mechanisms delivers a precise highly controlled energy dose that rapidly elevates tissue temperature and creates localized cell destruction. The MCT vastly reduces many of the hazarded associated with other energy-based treatments. As microwave energy travels into the tissue, the water molecules try to align with microwave field causing them to collide and create friction, the heat generated quickly destroyed all target tissues and creates a highly accurate zone of treatment within just few seconds.

There are other purposes of the phantoms, such as palpation to detect the pathological areas,[40] and it is considered helpful in the surgical field such as the vascular surgery,[83] timing reality simultaneous with US images,[84] development of a computerized 4-D MRI,[85] iron concentration level can be detected by biomagnetic liver susceptometry,[14,46] and development of coaxial ultrasonic probe for fatty liver diagnostic.[86]

Conclusion

In this review article, the materials that have been used in liver phantoms have been widely reviewed as alternatives to human tissues and were used for different targets. Furthermore, the considered factors for different modalities such as CT, US, gamma scintillation, and MRI were explained in detail. The article has also included the applications of liver phantoms in both diagnostic and therapeutic purposes.

Financial support and sponsorship

Nil.

Conflicts of interest

There are no conflicts of interest.

References

1. Wakim KG. Physiology of the liver. Am J Med 1954;16;256-71.
2. Brunetti A, Cuocolo A. European science foundation calls for more and better medical imaging research. Eur J Nucl Med Mol Imaging 2008;35:1749-57.
3. Qiu K, Haghiashtiani G, McAlpine MC. 3D printed organ models for surgical applications. Annu Rev Anal Chem (Palo Alto Calif) 2018;11:287-306.
4. Pacioni A, Carbone M, Freschi C, Viglialoro R, Ferrari V, Ferrari M. Patient-specific ultrasound liver phantom: Materials and fabrication method. Int J Comput Assist Radiol Surg 2015;10:1065-75.
5. Kondo T, Kitatuji M, Shikinami Y, Tuta K, Kanda H. New tissue mimicking materials for ultrasound phantoms. Proc IEEE Ultrason Symp 2005;3:1664-7.
6. Gear JI, Long C, Rushforth D, Chittenden SJ, Cummings C, Flux GD. Development of patient-specific molecular imaging phantoms using a 3D printer. Med Phys 2014;41:082502.
7. Singh S, Repaka R. Numerical study to establish relationship between coagulation volume and target tip temperature during temperature-controlled radiofrequency ablation. Electromagn Biol Med 2018;37:13-22.
8. De Luca F, Maraviglia B, Mercurio A. Biological tissue simulation and standard testing material for MRI. Magn Reson Med 1987;4:189-92.
9. Braun F, Schalk R, Heintz A, Feike P, Firmowski S, Beuermann T, *et al*. NADH-fluorescence scattering correction for absolute concentration determination in a liquid tissue phantom using a novel multispectral magnetic-resonance-imaging-compatible needle probe. Meas Sci Technol 2017;28:75903
10. Mathur-De Vre R, Grimee R, Parmentier F, Binet J. The use of agar gel as a basic reference material for calibrating relaxation times and

imaging parameters. Magn Reson Med 1985;2:176-9.
11. Christoffersson JO, Olsson LE, Sjöberg S. Nickel-doped agarose gel phantoms in MR imaging. Acta Radiol 1991;32:426-31.
12. Arif M, Moelker A, van Walsum T. Needle tip visibility in 3D ultrasound images. Cardiovasc Intervent Radiol 2018;41:145-52.
13. Krucker T, Lang A, Meyer EP. New polyurethane-based material for vascular corrosion casting with improved physical and imaging characteristics. Microsc Res Tech 2006;69:138-47.
14. Kao YH, Luddington OS, Culleton SR, Francis RJ, Boucek JA. A gelatin liver phantom of suspended 90Y resin microspheres to simulate the physiologic microsphere biodistribution of a postradioembolization liver. J Nucl Med Technol 2014;42:265-8.
15. Summers PE, Holdsworth DW, Nikolov HN, Rutt BK, Drangova M. Multisite trial of MR flow measurement: Phantom and protocol design. J Magn Reson Imaging 2005;21:620-31.
16. Casciaro S, Conversano F, Musio S, Casciaro E, Demitri C, Sannino A, *et al.* Full experimental modelling of a liver tissue mimicking phantom for medical ultrasound studies employing different hydrogels. J Mater Sci Mater Med 2009;20:983-9.
17. Leng S, Chen B, Vrieze T, Kuhlmann J, Yu L, Alexander A, *et al.* Construction of realistic phantoms from patient images and a commercial three-dimensional printer. J Med Imaging (Bellingham) 2016;3:033501.
18. Gear JI, Cummings C, Craig AJ, Divoli A, Long CD, Tapner M, *et al.* Abdo-man: A 3D-printed anthropomorphic phantom for validating quantitative SIRT. EJNMMI Phys 2016;3:17.
19. Lee MY, Han B, Jenkins C, Xing L, Suh TS. A depth-sensing technique on 3D-printed compensator for total body irradiation patient measurement and treatment planning. Med Phys 2016;43:6137.
20. Bücking TM, Hill ER, Robertson JL, Maneas E, Plumb AA, Nikitichev DI. From medical imaging data to 3D printed anatomical models. PLoS One 2017;12:e0178540.
21. In E, Walker E, Naguib HE. Novel development of 3D printable UV-curable silicone for multimodal imaging phantom. Bioprinting 2016;7:19-26.
22. Li JH, Tsai CY, Huang HM. Assessment of hepatic fatty infiltration using dual-energy computed tomography: A phantom study. Physiol Meas 2014;35:597-606.
23. FitzGerald PF, Colborn RE, Edic PM, Lambert JW, Bonitatibus PJ Jr., Yeh BM. Liquid tissue surrogates for X-ray and CT phantom studies. Med Phys 2017;44:6251-60.
24. Oglat AA, Matjafri MZ, Suardi N, Abdelrahman MA, Oqlat MA, Oqlat AA. A new scatter particle and mixture fluid for preparing blood mimicking fluid for wall-less flow phantom. J Med Ultrasound 2018;26:134-42.
25. Oglat AA, Matjafri MZ, Suardi N, Mostafa A. Acoustical and physical characteristic of a new blood mimicking fluid phantom acoustical and physical characteristic of a new blood mimicking fluid phantom. Journal of Physics: Conference Series 2018;1083. No. 1.
26. Euclid S. Computed tomography: Physical principles, clinical applications, and quality control. Elsevier Health Sciences, 2015.
27. Cherry S, Sorenson J, Phelps M. Physics in Nuclear Medicine. Elsevier Health Sciences, 2012.
28. Kim KS, Lee JM, Kim SH, Kim KW, Kim SJ, Cho SH, *et al.* Image fusion in dual energy computed tomography for detection of hypervascular liver hepatocellular carcinoma: Phantom and preliminary studies. Invest Radiol 2010;45:149-57.
29. Joe E, Kim SH, Lee KB, Jang JJ. Noninvasive determination of hepatic iron accumulation 1 purpose: Methods, results. Radiology 2012;262:126-35.
30. D'Souza WD, Madsen EL, Unal O, Vigen KK, Frank GR, Thomadsen BR. Tissue mimicking materials for a multi-imaging modality prostate phantom. Med Phys 2001;28:688-700.
31. Widmann G, Wallach D, Toporek G, Schullian P, Weber S, Bale R. Angiographic C-arm CT- versus MDCT-guided stereotactic punctures of liver lesions: Nonrigid phantom study. AJR Am J Roentgenol 2013;201:1136-40.
32. Schindera ST, Torrente JC, Ruder TD, Hoppe H, Marin D, Nelson RC, *et al.* Decreased detection of hypovascular liver tumors with MDCT in obese patients: A phantom study. AJR Am J Roentgenol 2011;196:W772-6.
33. Schindera ST, Nelson RC, Howle L, Nichols E, DeLong DM, Merkle EM. Effect of varying injection rates of a saline chaser on aortic enhancement in CT angiography: Phantom study. Eur Radiol 2008;18:1683-9.
34. Bush NL, Hill CR. Gelatine-alginate complex gel: A new acoustically tissue-equivalent material. Ultrasound Med Biol 1983;9:479-84.
35. Cook JR, Bouchard RR, Emelianov SY. Tissue-mimicking phantoms for photoacoustic and ultrasonic imaging. Biomed Opt Express 2011;2:3193-206.
36. Anderson PG, Rouze NC, Palmeri ML. Effect of graphite concentration on shear-wave speed in gelatin-based tissue-mimicking phantoms. Ultrason Imaging 2011;33:134-42.
37. Surry KJ, Austin HJ, Fenster A, Peters TM. Poly (vinyl alcohol) cryogel phantoms for use in ultrasound and MR imaging. Phys Med Biol 2004;49:5529-46.
38. Demitri C, Sannino A, Conversano F, Casciaro S, Distante A, Maffezzoli A. Hydrogel based tissue mimicking phantom for *in vitro* ultrasound contrast agents studies. J Biomed Mater Res B Appl Biomater 2008;87:338-45.
39. Anderson ME, Trahey GE. The direct estimation of sound speed using pulse-echo ultrasound. J Acoust Soc Am 1998;104:3099-106.
40. Fromageau J, Brusseau E, Vray D, Gimenez G, Delachartre P. Characterization of PVA cryogel for intravascular ultrasound elasticity imaging. IEEE Trans Ultrason Ferroelectr Freq Control 2003;50:1318-24.
41. Oglat AA, Matjafri MZ, Suardi N, Oqlat MA, Abdelrahman MA, Oqlat AA. A review of medical Doppler ultrasonography of blood flow in general and especially in common carotid artery. J Med Ultrasound 2018;26:3-13.
42. Oglat AA, Matjafri M, Suardi N, Oqlat MA, Oqlat AA, Abdelrahman MA. A new blood mimicking fluid using propylene glycol and their properties for a flow phantom test of medical doppler ultrasound. International Journal of Chemistry, Pharmacy & Technology 2017;2.5.
43. Ammar MS, Oglat A, Matjafri MZ, Suardi N. Chemical items used for preparing tissue-mimicking material of wall-less flow phantom for Doppler ultrasound imaging. J Med Ultrasound 2018;26:123.
44. Oglat AA, Matjafri MZ, Suardi N, Characterization and Construction of a Robust and Elastic Wall-Less Flow Phantom for High Pressure Flow Rate Using Doppler Ultrasound Applications. Nat Eng Sci 2018;3:3.
45. Rouyer J, Torres G, Amador C, Urban MW, Lavarello R. Simultaneous estimation of shear elastic modulus and backscatter coefficient: Phantom and in human liver *in vivo* study. IEEE Int Ultrason Symp IUS 2016;2016:16-9.
46. Ahmad MS, Kabir NA, Nursakinah S, Oglat AA, Thabit HA, Zeyadeh SL, Radioluminescence and scintillation properties of zinc doped with aluminum. Int J Chem Pharm Technol 2018;3:44-9.
47. Hunt DC, Easton H, Caldwell CB. Design and construction of a quality control phantom for SPECT and PET imaging. Med Phys 2009;36:5404-11.
48. Walrand S, Hesse M, Demonceau G, Pauwels S, Jamar F. Yttrium-90-labeled microsphere tracking during liver selective internal radiotherapy by bremsstrahlung pinhole SPECT: Feasibility study and evaluation in an abdominal phantom. EJNMMI Res 2011;1:32.
49. Elschot M, Nijsen JF, Dam AJ, de Jong HW. Quantitative evaluation of scintillation camera imaging characteristics of isotopes used in liver radioembolization. PLoS One 2011;6:e26174.
50. De Mello JQ, Lucena EA, Dantas AL, Dantas BM. Development and evaluation of a technique for *in vivo* monitoring of ^{60}Co in human lungs. J Phys Conf Ser 2016;733:1-4.
51. Barrett HH, Yao J, Rolland JP, Myers KJ. Model observers for assessment of image quality. Proc Natl Acad Sci U S A 1993;90:9758-65.
52. Yoshimura K, Kato H, Kuroda M, Yoshida A, Hanamoto K, Tanaka A, *et al.* Development of a tissue-equivalent MRI phantom using carrageenan gel. Magn Reson Med 2003;50:1011-7.
53. Tofts PS. Quality assurance: Accuracy, precision, controls and phantoms.In: Quantitative MRI of the Brain. Department of Radiology Medical University of South Carolina: CRC Press; 2018. p. 33-54.
54. Mano I, Goshima H, Nambu M, Iio M. New polyvinyl alcohol gel material for MRI phantoms. Magn Reson Med 1986;3:921-6.
55. Cho GY, Kim S, Jensen JH, Storey P, Sodickson DK, Sigmund EE.

A versatile flow phantom for intravoxel incoherent motion MRI. Magn Reson Med 2012;67:1710-20.
56. Chmarra MK, Hansen R, Mårvik R, Langø T. Multimodal phantom of liver tissue. PLoS One 2013;8:e64180.
57. Blechinger JC, Madsen EL, Frank GR. Tissue-mimicking gelatin-agar gels for use in magnetic resonance imaging phantoms. Med Phys 1988;15:629-36.
58. Lee SS, Lee Y, Kim N, Kim SW, Byun JH, Park SH, *et al.* Hepatic fat quantification using chemical shift MR imaging and MR spectroscopy in the presence of hepatic iron deposition: Validation in phantoms and in patients with chronic liver disease. J Magn Reson Imaging 2011;33:1390-8.
59. Rethy A, Sæternes JO, Halgunset J, Mårvik R, Hofstad EF, Sánchez-Margallo JA, *et al.* Anthropomorphic liver phantom with flow for multimodal image-guided liver therapy research and training. Int J Comput Assist Radiol Surg 2018;13:61-72.
60. Vernon ML, Freàchette J, Painchaud Y, Caron S, Beaudry P. Fabrication and characterization of a solid polyurethane phantom for optical imaging through scattering media. Appl Opt 1999;38:4247-51.
61. Kato H, Kuroda M, Yoshimura K, Yoshida A, Hanamoto K, Kawasaki S, *et al.* Composition of MRI phantom equivalent to human tissues. Med Phys 2005;32:3199-208.
62. Patil S, Burgner J, Webster RJ 3rd, Alterovitz R. Needle steering in 3-D via rapid replanning. IEEE Trans Robot 2014;30:853-64.
63. Investigation of the effect of kV combinations on image quality for virtual monochromatic imaging using dual-energy CT: A phantom study. J Radiat Prot Res 2018;43:1-9.
64. Li JH, Du YM, Huang HM. Accuracy of dual-energy computed tomography for the quantification of iodine in a soft tissue-mimicking phantom. J Appl Clin Med Phys 2015;16:418-26.
65. Wang S, Cao X, Sun X, Zhang B, Xie Q, Xiao P. Anatomical information based panel PET image reconstruction using nonlocal means regularization. 2015 IEEE Nuclear Science Symposium and Medical Imaging Conference (NSS/MIC). IEEE, 2015.
66. Große Hokamp N, Höink AJ, Doerner J, Jordan DW, Pahn G, Persigehl T, *et al.* Assessment of arterially hyper-enhancing liver lesions using virtual monoenergetic images from spectral detector CT: Phantom and patient experience. Abdom Radiol (NY) 2018;43:2066-74.
67. Yoon JH, Lee JM, Hur BY, Baek J, Shim H, Han JK, *et al.* Influence of the adaptive iterative dose reduction 3D algorithm on the detectability of low-contrast lesions and radiation dose repeatability in abdominal computed tomography: A phantom study. Abdom Imaging 2015;40:1843-52.
68. Manescu P, Ladjal H, Azencot J, Beuve M, Shariat B. Motion compensation for PET image reconstruction using deformable tetrahedral meshes. Phys Med Biol 2015;60:9269-93.
69. Mulabecirovic A, Mjelle AB, Gilja OH, Vesterhus M, Havre RF. Repeatability of shear wave elastography in liver fibrosis phantoms-evaluation of five different systems. PLoS One 2018;13:e0189671.
70. Schenk JP, Alzen G, Klingmüller V, Teufel U, El Sakka S, Engelmann G, *et al.* Measurement of real-time tissue elastography in a phantom model and comparison with transient elastography in pediatric patients with liver diseases. Diagn Interv Radiol 2014;20:90-9.
71. Porter CA, Bradley KM, Hippeläinen ET, Walker MD, McGowan DR. Phantom and clinical evaluation of the effect of full monte carlo collimator modelling in post-SIRT yttrium-90 bremsstrahlung SPECT imaging. EJNMMI Res 2018;8:7.
72. Shimohigashi Y, Araki F, Maruyama M, Yonemura K, Nakaguchi Y, Kai Y, *et al.* Image quality of four-dimensional cone-beam computed tomography obtained at various gantry rotation speeds for liver stereotactic body radiation therapy with fiducial markers. Phys Med 2018;45:19-24.
73. Followill DS, Evans DR, Cherry C, Molineu A, Fisher G, Hanson WF, *et al.* Design, development, and implementation of the radiological physics center's pelvis and thorax anthropomorphic quality assurance phantoms. Med Phys 2007;34:2070-6.
74. Gallo JJ, Kaufman I, Powell R, Pandya S, Somnay A, Bossenberger T, *et al*. Single-fraction spine SBRT end-to-end testing on TomoTherapy, Vero, TrueBeam, and CyberKnife treatment platforms using a novel anthropomorphic phantom. J Appl Clin Med Phys 2015;16:5120.
75. Gallo JJ, Kaufman I, Powell R, Pandya S, Somnay A, Bossenberger T, *et al*. Single-fraction spine SBRT end-to-end testing on tomotherapy,vero, truebeam, and cyberknife treatment platforms using a novel anthropomorphic phantom. J Appl Clin Med Phys 2017;16:170-82.
76. Oglat AA, Suardi N, Matjafri MZ, Oqlat MA, Abdelrahman MA, Oqlat AA. A review of suspension-scattered particles used in blood-mimicking fluid for Doppler ultrasound imaging. J Med Ultrasound 2018;26:68-76.
77. Mikhail AS, Negussie AH, Graham C, Mathew M, Wood BJ, Partanen A, *et al.* Evaluation of a tissue-mimicking thermochromic phantom for radiofrequency ablation. Med Phys 2016;43:4304.
78. Li K, Su Z, Xu E, Huang Q, Zeng Q, Zheng R. Evaluation of the ablation margin of hepatocellular carcinoma using CEUS-CT/MR image fusion in a phantom model and in patients. BMC Cancer 2017;17:61.
79. Paolucci I, Schwalbe M, Prevost GA, Lachenmayer A, Candinas D, Weber S, *et al.* Design and implementation of an electromagnetic ultrasound-based navigation technique for laparoscopic ablation of liver tumors. Surg Endosc 2018;32:3410-9.
80. Freesmeyer M, Winkens T, Kühnel C. Real-time handheld emission spot allocator (rthESA) for simultaneous fusion imaging with ultrasound. Nuklearmedizin 2014;53:265-71.
81. Eisele RM. Advances in local ablation of malignant liver lesions. World J Gastroenterol 2016;22:3885-91.
82. Zhai F, Nan Q, Ding J, Xu D, Zhang H, Liu Y, *et al.* Comparative experiments on phantom and *ex vivo* liver tissue in microwave ablation. Electromagn Biol Med 2015;34:29-36.
83. Zhou X, Kenwright DA, Wang S, Hossack JA, Hoskins PR. Fabrication of two flow phantoms for Doppler ultrasound imaging. IEEE Trans Ultrason Ferroelectr Freq Control 2017;64:53-65.
84. Michael A, John R, Michael D. The development of a minimally invasive radiofrequency ablation coil electrode. CMBES Proceedings 2018;4:10-3.
85. Wang C, Yin FF, Segars WP, Chang Z, Ren L. Development of a Computerized 4-D MRI Phantom for Liver Motion Study. Technol Cancer Res Treat 2017;16:1051-9.
86. Hori M, Yokota D, Aotani Y, Kumagai Y, Wada K, Matsunaka T, *et al*. Development of coaxial ultrasonic probe for fatty liver diagnostic system using ultrasonic velocity change. Jpn J Appl Phys 2017;56:7-10.